Available online at www.eccomasproceedia.org
Eccomas Proceedia COMPDYN (2023) 9-23

ECCOMAS
Proceedia

COMPDYN 2023
9th ECCOMAS Thematic Conference on
Computational Methods in Structural Dynamics and Earthquake Engineering
M. Papadrakakis, M. Fragiadakis (eds.)
Athens, Greece, 12-14 June 2023

SEISMIC PROTECTION OF SUBSTANDARD RC FRAMES THROUGH SELF-CENTERING DISSIPATIVE BRACES

Dario De Domenico[1], Luca Facconi[2], Emanuele Gandelli[2,*], Alberto Gioitta[1], Paolo Longo[1], Natale Maugeri[1]

[1] Department of Engineering, University of Messina,
Contrada Di Dio, 98166, Sant'Agata, Messina, Italy
{dario.dedomenico, paolo.longo, natale.maugeri}@unime.it, albertogioitta@gmail.com

[2] Department of Civil, Environmental, Architectural Engineering and Mathematics (DICATAM),
University of Brescia, Via Branze, 43, 25123, Brescia, Italy
e-mail: {emanuele.gandelli, luca.facconi}@unibs.it

Abstract

Several existing reinforced concrete (RC) framed buildings require urgent retrofit interventions to meet modern seismic-performance requirements because of poor construction details, increased seismic hazard, change of intended use over their service life, or occurrence of material degradation phenomena. Furthermore, these structures were designed considering outdated principles or even totally ignoring the seismic action. Among the possible retrofit strategies, an effective technique implies the use of metallic dampers installed in chevron braces and optimally distributed in the structure to provide supplemental energy dissipation (and stiffening) effects. However, such conventional elasto-plastic dissipative braces (EPDBs) may suffer from recentering issues, because their working mechanism is, in general cases, based on the plastic deformation of steel. Consequently, they exhibit permanent displacements at the end of the seismic event and need to be restored after each shaking. As an alternative, this contribution deals with the seismic protection of existing RC buildings through self-centering dissipative braces (SCDBs) that are featured by internal mechanisms nullifying the permanent deformation after their activation, thus offering significant advantages over EPDBs. We present a displacement-based design procedure for SCDBs implemented in RC framed structures targeting two performance requirements, namely the control of the roof displacement and the good recentering behavior of the structure after the seismic event. Then, we apply this procedure to the seismic protection of an archetypal building, representative of substandard RC frames built in 1960s-1970s in Italy, by comparatively illustrating the seismic performance of SCDBs and EPDBs through nonlinear time-history analyses.

Keywords: Self-centering dissipative braces, Seismic protection, Reinforced concrete frames, Elasto-plastic dissipative braces, Displacement-based seismic design, Recentering behavior.

ISSN:2623-3347
Peer-review under responsibility of the organizing committee of COMPDYN 2023.
doi: 10.7712/120123.10382.20472

1 INTRODUCTION

Existing reinforced concrete (RC) framed structures, built more 40-50 years ago, were conceived upon outdated design regulations, and do not meet performance requirements of current seismic standards [1], [2]. A local intervention, e.g., applying composite systems [3], [4] to weaker zones or similar strengthening techniques, is often uneconomical for large-size buildings because of the high number of beam and column elements involved. As an alternative, substandard RC structures can be retrofitted through a relatively low number of dampers [5]-[7], which are deployed in specific locations of the framed structure to provide supplemental energy dissipation (and stiffening) effects. One of the most common typologies is represented by conventional *elasto-plastic dissipative braces* (EPDBs) realized with metallic dampers, which rely on the stable yielding mechanism offered by ductile steel members [8], [9]. These members are purposely designed to undergo large plastic deformation during the seismic event, thus absorbing most of the earthquake-induced input energy through internal hysteretic mechanisms while reducing the seismic damage in the RC frame. In other words, they behave as "fuse elements" and, naturally, suffer from permanent displacements at the end of the seismic event (especially under severe seismic excitations). This implies that, although the parent RC framed structure can be efficiently protected during the design earthquake, such dampers should be replaced or, anyway, restored after each shaking. As a more efficient strategy, *self-centering dissipative braces* (SCDBs) incorporate internal mechanisms to reduce (or totally eliminate) residual displacements upon their engagement and, consequently, offer significant advantages over EPDBs. Such technology was historically implemented through superelastic properties of shape memory alloys (SMAs) [10]-[12], which are expensive materials. Cheaper alternatives to obtain a flag-shaped hysteretic behavior have been introduced in the market more recently, e.g., those exploiting pre-compressed metallic springs or based on the relative sliding of mating metallic parts along inclined surfaces [13]-[17]. Although these solutions have been promisingly implemented in sporadic case-study projects, a systematic design procedure for the seismic retrofit of substandard RC frames through SCDBs is missing in the literature. These are the motivations of this contribution, which presents a linear displacement-based design procedure [18], of general applicability, for SCDBs implemented in RC framed structures and targeting two performance criteria, namely the control of the roof displacement and the absence of residual inter-storey drifts at the end of the seismic event. The latter target is accomplished by suitably selecting the re-centering force of the SCDBs at each storey level depending on reinforcement configuration and axial load ratio of RC columns. The proposed procedure is then applied to an archetypal building, representative of substandard RC frames built in 1960s-1970s in Italy [19]-[22]. The seismic performance of such case-study building, protected by either EPDBs or SCDBs, is evaluated through nonlinear time-history analyses and comparatively discussed to demonstrate the main advantages of the proposed seismic protection strategy in terms of developed collapse mechanism and residual displacement at the end of the seismic event.

2 MOTIVATIONS AND PRELIMINARY CONCEPTS

In Italy, many existing RC buildings were realized with outdated or non-seismic criteria, especially those constructed in 1970s. These structures, in some emblematic cases, were designed taking into consideration gravity loads only, without any concern regarding seismic action. These structures are, in fact, characterized by low amounts of transverse reinforcement in beam and column members, lack of capacity design principles, poor construction details, etc. Moreover, the seismic risk map has evolved over the past decades, and locations that had been previously considered as non-seismic areas are nowadays characterized by low-to-

moderate seismic risk. Therefore, it is of utmost importance to elaborate efficient and practical techniques to retrofit substandard RC buildings with regard to seismic loading. Apart from the aforementioned increased seismic hazard in the installation site of existing buildings, other motivations behind a seismic retrofit strategy are the material degradation phenomena that inherently take place in RC structures, like corrosion of reinforcing bars and resulting spalling and microcracking of concrete cover, loss of bond strength at the steel-concrete interface, and reduction of confinement effects of stirrups [23].

Traditional supplemental energy dissipation devices like metallic or friction dampers involved in EPDBs exploit the plastic deformation of steel to dissipate a certain portion of the earthquake-induced input energy, thus considerably reducing the vibrational energy, the hysteretic energy and, as a result, the expected damage of the parent structure. Typical force-displacement cycles of EPDBs are depicted in Figure 1 (left), where two possible behaviors (elastic-perfectly plastic and elasto-plastic with slight hardening $k_p > 0$) are presented. At the end of the ground motion, the EPDBs suffer from non-zero residual displacements due to the accumulated plastic deformation. This, in turn, generates a poor recentering behavior of the overall structure, due to the fact that these fuse elements are permanently displaced. After a seismic event, the structure can be brough back to its original position by externally applying a force, which is always costly. Additionally, as the dampers themselves have accumulated permanent displacement during a main shock, their residual stroke is reduced, and they might not behave as expected for aftershock events and seismic sequences. As an alternative, in recent years many devices have been developed to incorporate an internal recentering mechanism in so-called self-centering dampers which are installed in SCDBs and are characterized by negligible residual displacements, thus offering significant advantages over EPDBs. The peculiar flag-shaped force-displacement cycle in Figure 1 (right) could be obtained in different manners, e.g., by means of post-tensioned tendons, preloaded spring dampers, exploiting the superelastic properties of SMAs, or through innovative sliding friction devices. Just as a representative example, the device sketched in Figure 1 (right) is called *Resilient Slip Friction Joint* (RSFJ), was patented in 2016 [24] and has already been installed in several civil engineering projects, like the Nelson airport in Nelson, New Zealand and the 2150 Keith Drive all-timber brace frame building in Vancouver, Canada, to name just a couple. The RSFJ exploits Belleville springs (conical disc springs) that act, through high-strength bolts, on grooves featured by a certain inclination angle. Such angle is specifically designed to achieve the self-centering behavior of the device: indeed, upon unloading, the elastic force induced by the Belleville springs when the slotted plates are moved from their original position exceeds the resisting friction force of between the plate surfaces and, consequently, automatically re-center the device.

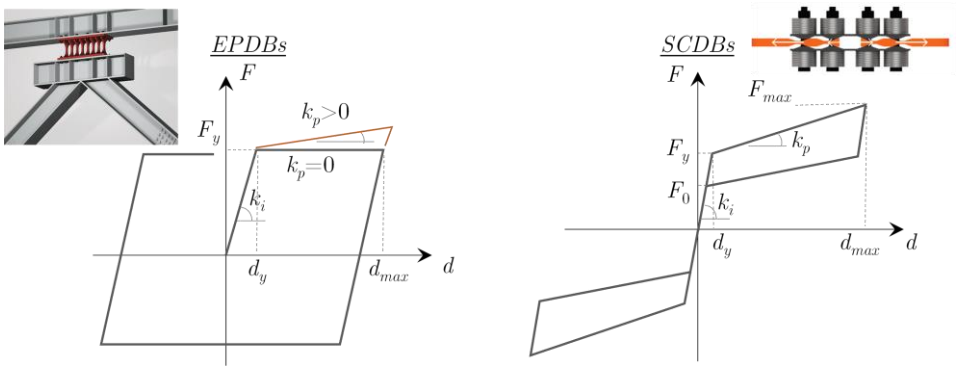

Figure 1: Schematic comparison of force-displacement cycle of EPDBs and SCDBs

Despite the appealing properties of the above-mentioned RSFJs, in this contribution we purposely omit going into the specific details of the constructive technology used to accomplish the flag-shaped behavior in Figure 1 (right). On the contrary, we investigate the seismic performance of substandard RC buildings equipped with SCDBs in general terms, implicitly meaning that the force-displacement cycle is characterized by a yielding force F_y (force at the beginning of the slip), a maximum force F_{max} and a residual force upon unloading F_0 (force at the end of the slip), an initial stiffness k_i (i.e., before slip) and a post-slip stiffness k_p as shown in Figure 1 (right).

3 DESIGN PROCEDURE OF SCDBS FOR RC FRAMES

A linear displacement-based design procedure for SCDBs implemented in RC framed structures is adopted in this work, which addresses two performance requirements, namely the control of the roof displacement that should match a target, predefined value (selected in relationship to the importance of the structure and its intended use), and the good recentering behavior of the structure, quantified via the maximum residual displacement among the ones observed at each storey level after the seismic event.

The design procedure consists of the following steps:

1) Perform a nonlinear static (pushover) analysis on the RC frame. Define an equivalent single-degree-of-freedom (SDOF) system through an elastic-perfectly plastic bilinearization of the capacity curve as per Annex B of Eurocode 8 [2] based on the modal participation factor at the first mode Γ_1. All the quantities related to the equivalent SDOF will be denoted through a superscript *. The yielding force $F^*_{F,y}$, yielding displacement $d^*_{F,y}$ (and, consequently, the elastic stiffness $k^*_{F,el} = F^*_{F,y}/d^*_{F,y}$) and ultimate displacement $d^*_{F,u}$ of the RC frame are the output variables of the pushover analysis. The participating mass in the first modal shape is the mass M^*_F of the equivalent SDOF.
2) Based on the pushover results, determine the yielding force $F_{F,y,i}$, the corresponding yielding drift $\Delta_{y,i}$ and the elastic stiffness at each storey level i (i=1, 2, …, n).
3) Based on the reinforcement layout of the beam-column members and the axial force of the columns at each storey level i, it is possible to determine the value of force at zero displacement for the i^{th} storey $F_{F,0,i}$. In particular, this value has been obtained in a separate parametric study, carried out by the authors and only briefly mentioned here for the sake of brevity, through a series of cyclic pushover analyses covering a range of longitudinal reinforcement ratio $\rho_{l,i}$, transverse reinforcement ratios $\rho_{s,i}$, and axial load ratios ALR_i of practical interest in real existing RC buildings. The nonlinear frame models considered in this parametric study incorporate material nonlinearity through a fiber hinge approach, with a Pivot hysteretic model [25] at the fiber level to describe possible pinching effects ascribed to weak transverse reinforcement and poor construction details that might be observed in existing RC structures (Figure 2). The value $F_{F,0,i}$ is of utmost importance for RC structures because the SCDBs should be designed to have a force at zero displacement $F_{DB,0,i} > F_{F,0,i}$ in order to guarantee the recentering behavior. The average value of the ratios $F_{F,0,i}/F_{F,y,i}$ for the various storeys is assumed as the ratio $F^*_{F,0}/F^*_{F,y}$ representative of the equivalent SDOF in the design procedure.
4) Select the target displacement of the frame retrofitted with SCDBs d^*_{target} (in general cases, one could assume $d^*_{F,y} \leq d^*_{target} \leq d^*_{F,u}$). Based on d^*_{target}, determine the ductility parameter $\mu^*_F = d^*_{target}/d^*_{F,y}$ and the effective stiffness of the equivalent SDOF as $k^*_{F,eff} = k^*_{F,el}/\mu^*_F$. Based on $T^*_{F,eff} = 2\pi\,(M^*_F/k^*_{F,eff})^{0.5}$ and μ^*_F, one can estimate the hysteretic damping of the equivalent SDOF $\xi^*_{F,hyst}$ through empirical formulae from the literature [26], depending on the observed hysteretic shape. A small Takeda (for $F^*_{F,0}/F^*_{F,y} <$

0.35) or a large Takeda (for $F^*_{F,0}/F^*_{F,y} \geq 0.35$) hysteresis model can be assumed, depending on the energy dissipation capability.

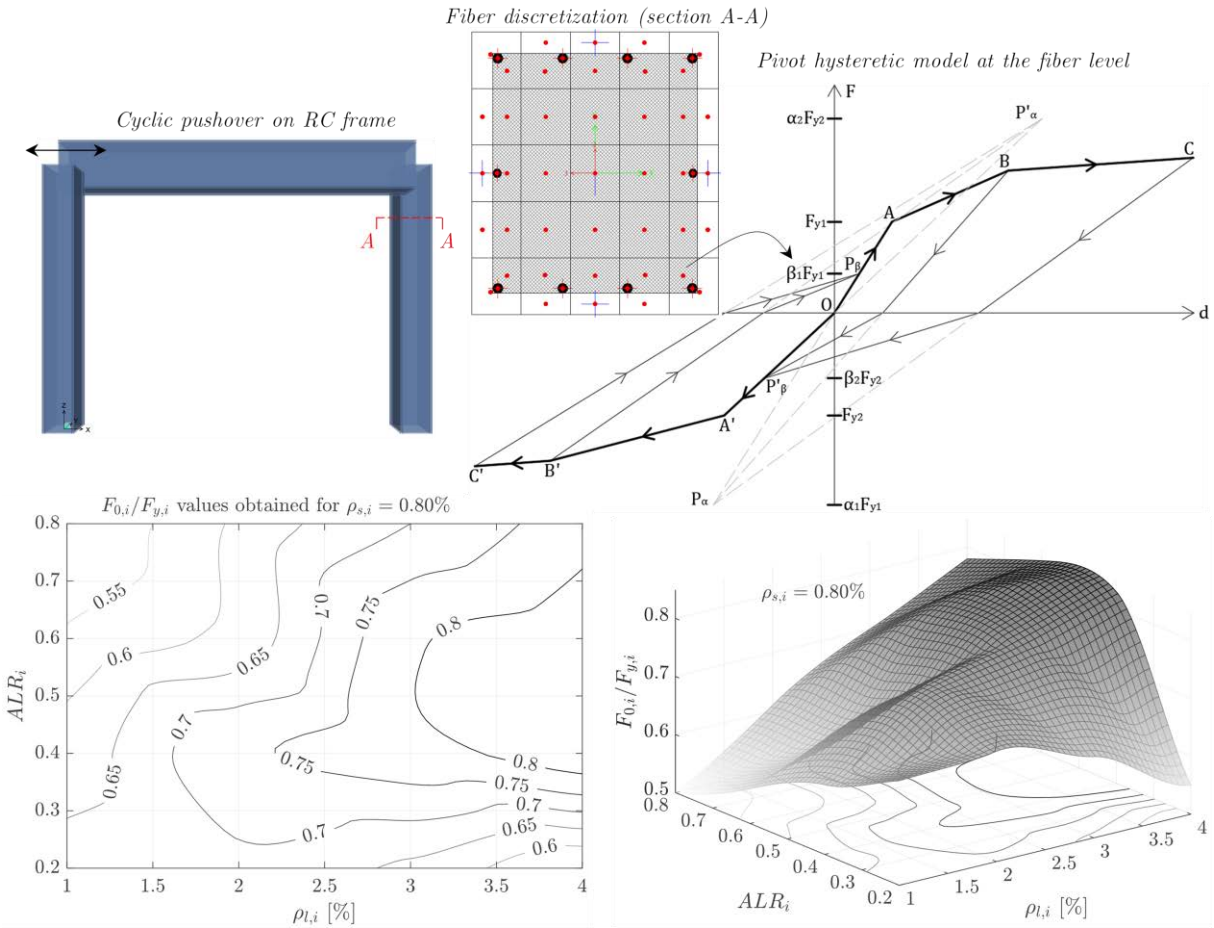

Figure 2: Pivot hysteretic model at the fiber level adopted in the parametric study to determine $F_{F,0,i}$ (top) and contour and surface plots of the $F_{F,0,i}/F_{F,y,i}$ ratios obtained for an arbitrary set of frame parameters (bottom)

5) Similar to the RC frame, the SCDBs are designed through an equivalent SDOF concept characterized by a yielding force $F^*_{DB,y}$ (at the beginning of the slip), a force at zero displacement $F^*_{DB,0}$ (at the end of the slip), a post-slip stiffness $k^*_{DB,pl}$ and a ductility index μ^*_{DB}. Preliminarily, it is verified that $F^*_{DB,y} \geq F^*_{F,y}$. The recentering behavior is ensured by imposing $F^*_{DB,0} \geq F^*_{F,0}$ determined at the step 3). The ductility index μ^*_{DB} is fixed in the range 10-15, based on conventional practice. The yielding displacement of the equivalent SDOF of the dissipative brace is then obtained as $d^*_{DB,y} = d^*_{target}/\mu^*_{DB}$, hence the elastic stiffness is given by $k^*_{DB,el} = F^*_{DB,y}/d^*_{DB,y}$, and the displacement at the end of the slip is $d^*_{DB,0} = F^*_{DB,0}/k^*_{DB,el}$.
6) Based on d^*_{target}, selected at step 4), and μ^*_{DB}, selected at step 5), one can estimate the effective stiffness and hysteretic damping of the dissipative brace. Indeed, the force at the target displacement is $F^*_{DB,dTarget} = F^*_{DB,y} + k^*_{DB,pl}\,(d^*_{target} - d^*_{DB,y})$, and then the effective stiffness is $k^*_{DB,eff} = F^*_{DB,dTarget}/d^*_{target}$; the hysteretic damping of the dissipative brace $\xi^*_{DB,hyst}$ is estimated through empirical formulae from the literature [26], assuming in this case a ring-spring hysteresis model due to the inherent flag-shape behavior.
7) The performance point in the acceleration-displacement response spectrum (ADRS) are obtained by combining stiffness and damping parameters of the frame and dissipative brace acting in parallel. In particular, the effective stiffness of the combined system is:

$k^*_{F+DB,eff} = k^*_{F,eff} + k^*_{DB,eff}$ and the corresponding period is $T^*_{F+DB,eff} = 2\pi (M^*_F/k^*_{F+DB,eff})^{0.5}$. The equivalent viscous damping of the frame + dissipative brace system is computed according to recommendations by Priestley et al. [18] as follows:

$$\xi^*_{F+DB,eq} = \xi^*_{F,el} + \frac{\xi^*_{F,hyst} \cdot F^*_{F,y} + \xi^*_{DB,hyst} \cdot F^*_{DB,y}}{F^*_{F,y} + F^*_{DB,y}} \quad (1)$$

where $\xi^*_{F,el}$ is the equivalent viscous damping of the frame, generally assumed as 0.05.

8) Based on $T^*_{F+DB,eff}$ and $\xi^*_{F+DB,eq}$, one can evaluate a new value of displacement directly from the damped displacement response spectrum S_d (obtained from the elastic response spectrum upon application of the damping reduction factor η proposed by Priestley et al. [18]) corresponding to the value of period $T^*_{F+DB,eff}$, that is $S^*_{d,F+DB}(T^*_{F+DB,eff}, \xi^*_{F+DB,eq})$. Such value $S^*_{d,F+DB}$ might be different from the target displacement d^*_{target} at the generic iteration k, therefore the procedure is repeated again from step 4) by assuming for the k+1 iteration a new target displacement $d^{*(k+1)}_{target} = S^{*(k)}_{d,F+DB}$ until a convergence criterion is reached.
9) Once convergence in step 8) is fulfilled, the procedure is concluded by distributing the forces and the stiffness coefficients of the dissipative braces according to the proportional criteria proposed by Di Cesare et al. [27].

The procedure illustrated above can be implemented in a simple spreadsheet and makes it possible to determine the mechanical properties and the height-wise distribution of the SCDBs to fulfill two performance requirements, namely the roof target displacement and the recentering behavior. This procedure is applied in the next section to a case study RC frame.

4 COMPARATIVE SEISMIC PERFORMANCE OF SCDBS AND EPDBS

The aim of this Section is to assess the seismic performance of SCDBs, designed according to the procedure described above, when implemented in existing RC frames, and compare this performance to that obtained by traditional EPDBs. For consistency reasons, the comparison between SCDBs and EPDBs is, of course, performed on the same structure and considering the same target displacement under the same seismic input, in terms of maximum roof displacement d_{max} and residual displacement d_r at the end of the seismic event.

4.1 Gravity-load design RC building selected as case study

The procedure is applied to an RC building representative of the Italian building stock of the 1970s. In particular, the 8-storey RC framed structure presented by Masi & Vona [19] is selected. This building has an inter-storey height of 3.0 m (total height equal to 24.0 m), three spans (length 5.0 m) in the analyzed (x) direction and was designed to resist gravity loads only according to the D.M. 30/05/1972 standards [28], namely permanent loads G = 5.0 kN/m^2 (reduced to 4.0 kN/m^2 at the roof level), and live loads Q = 2.0 kN/m^2. With regard to the cross sections and reinforcement details, columns have dimensions 30 x 30 cm at all storeys except the first storey (30 x 40 cm), and are reinforced with only four corner longitudinal bars of diameter Φ16 at the first storey, Φ14 at the second storey, and Φ12 from the third storey upward, and transverse reinforcement consisting of stirrups Φ6/15 cm at all storey levels. RC beams have section 30 x 50 cm and are reinforced with longitudinal bars 2Φ12 at the bottom and 5Φ12 at the top, and transverse reinforcement consisting of stirrups Φ6/25 cm. With regard to materials, concrete C20/25 grade, and steel A38 are considered. Considering the cross-section characteristics and the poor reinforcement details, this RC frame can be considered as an archetypal building representative of substandard RC frames built in 1960s-1970s in Italy and that, consequently, are in need of seismic retrofitting interventions.

4.2 Definition of seismic input

The design procedure of SCDBs (and of EPDBs) is implemented considering an installation site in Lamezia Terme (southern Italy, longitude 16.18°, latitude 38.58°), ground type C, nominal life 100 years, importance class IV, life safety limit state (SLV – return period 1898 years for a probability of exceedance equal to 10%). These parameters correspond to a high seismic hazard for a strategic structure. However, considering that the considered RC frame was originally designed for gravity loads only, it is unreasonable to assume such sever seismic excitation. Consequently, a scaling factor 0.48 was applied to obtain a more realistic seismic excitation to be considered in the design procedure (resulting peak ground acceleration equal to 0.219 g, g being the acceleration of gravity). A set of seven natural records have been selected through the software REXEL v.3.5 [29] and scaled in amplitude to be spectrum-compatible with the elastic response spectrum of the site in the range of periods 0.15-4.00 sec, as shown in Figure 3. The records have been selected from the European Strong-Motion Database considering moment magnitude M_w = 5-8 and epicentral distance R_{ep} = 30-100 km.

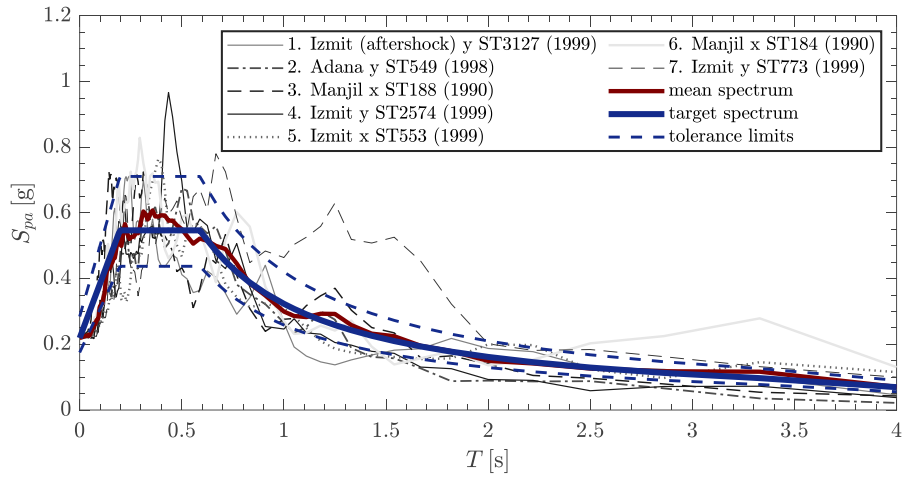

Figure 3: Elastic response spectrum of the site and spectrum matching for seven selected natural records

4.3 Numerical seismic performance evaluated through NLTHAs

The seismic performance is numerically evaluated through nonlinear time history analyses (NLTHAs) on a planar model of the RC building through the structural analysis software SAP2000 v. 21 [30]. A concentrated plasticity approach (with automatic hinge properties) has been adopted at either end of the beam-column members to incorporate material nonlinearity, according to the recommendations given in ASCE 41–17 [31]. The hinges are located at the 5% and 95% of the entire length of the structural members: moment-type plastic hinges have been adopted for RC beams as per Table 10-7 in ASCE 41–17 [31]; coupled axial-moment plastic hinges have been adopted for RC columns as per Table 10-8 in ASCE 41–17 [31]. A pivot hysteresis model has been adopted for both beam and columns, with parameters calibrated according to the recommendations by Sharma et al. [32] depending on the reinforcement layout and axial load ratio. The SCDBs are designed according to the procedure explained in Section 3, while the EPDBs are designed according to a classical displacement-based design procedure (see e.g., the procedure illustrated by Gandelli et al. [14]).

A preliminary pushover analysis is conducted on the RC building (without dampers) to determine strength and ductility parameters of the bare frame: based on the first modal participation factor Γ_1 = 1.29 and the capacity curve in Figure 4, the following results are obtained: $F^*_{F,y}$ =44.5 kN, $d^*_{F,y}$ = 13.1 mm, $d^*_{F,u}$ = 29.1 mm, maximum ductility $\mu^*_{F,max} = d^*_{F,u}/d^*_{F,y}$ = 2.2.

It is evident that the RC building has poor ductility characteristics and low deformation capacity. It is also worth noting that the building collapse is ascribed to a soft-storey mechanism at the third level (see again Figure 4). This result confirms that the structure was designed with regard to gravity loads only, without consideration to capacity design principles and strength hierarchy criteria (targeting a global collapse mechanism). It is reasonably expected that the introduction of dissipative braces (be them EPDBs or SCDBs) will certainly increase the deformation capacity, much beyond the value of $d_{F,u} = d^*_{F,u}\,\Gamma_1 = 37.5$ mm of the bare frame. Hence, in the design procedure of the dissipative braces, the target displacement has been assumed as $d_{target} = 120$ mm (roof displacement of the 8-storey RC building), which roughly corresponds to a 0.5% total drift of the structure. It is worth noting that this value corresponds to an average inter-storey drift of 0.5%, which is the threshold fixed by the Italian Building Code NTC2018 [1] as basic requirement for the Immediate Occupancy (IO) performance level, and is also a drift limitation adopted by other international standards as repairability threshold for unreinforced masonry infill and partition walls, such as SEAOC Vision 2000 [33], FEMA 356 [34] and ASCE/SEI 41 [31]. The final target displacement of the equivalent SDOF ($\Gamma_1 = 1.29$) at convergence of the iterative procedure (for the assumed response spectrum in Figure 3) is $d^*_{target} = 86.4$ mm, which is assumed as a common value for the design of both EPDBs and SCDBs. The resulting actual ductility index of the RC frame with SCDBs is $\mu^*_F = d^*_{target}/d^*_{F,y} = 6.6$. The elastic stiffness of the equivalent SDOF is $k^*_{F,el} = F^*_{F,y}/d^*_{F,y} = 3.4$ kN/mm, based on which the effective stiffness is $k^*_{F,eff} = k^*_{F,el}/\mu^*_F = 0.5$ kN/mm.

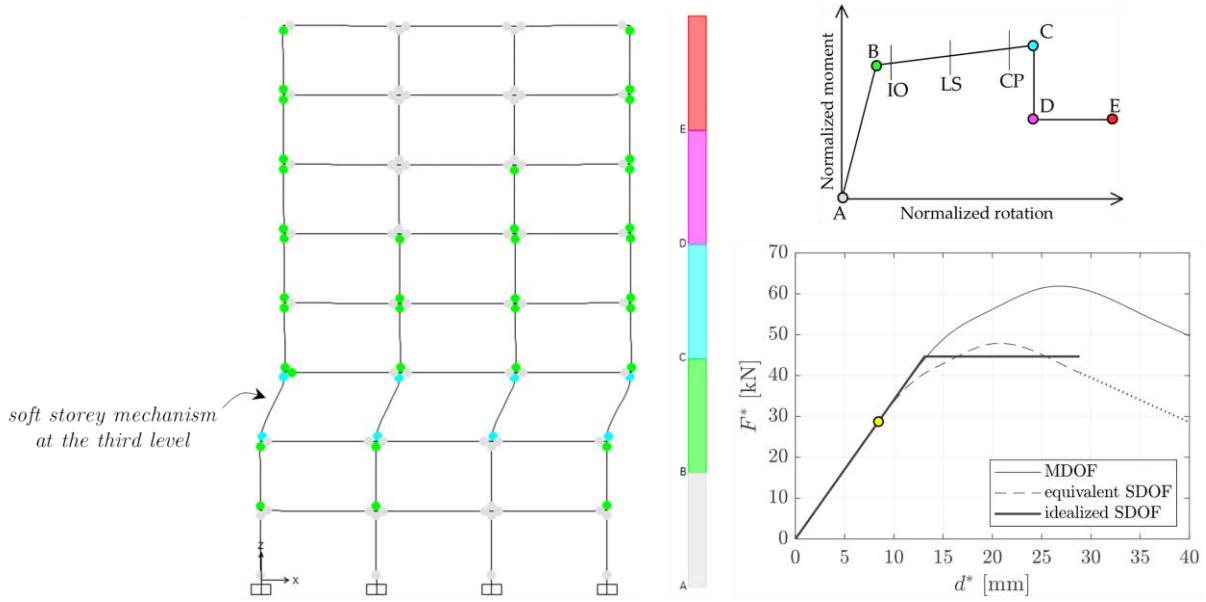

Figure 4: Pushover analysis on the bare RC frame and identification of collapse mechanism

The dissipative elements are then designed according to the procedure in Section 3, step 4). The dampers are implemented in the central bay and distributed along the building height through a chevron-brace configuration according to the layout in Figure 5 (left). A ductility index $\mu^*_{DB} = 12$ has been selected, while the yielding force $F^*_{DB,y} = 125$ kN and the force at zero displacement $F^*_{DB,0} = 25$ kN, from which the yielding displacement $d^*_{DB,y} = d^*_{target}/\mu^*_{DB} = 7.2$ mm, and the elastic stiffness $k^*_{DB,el} = F^*_{DB,y}/d^*_{DB,y} = 17.4$ kN/mm. Assuming a conventional post-elastic stiffness ratio $k^*_{DB,pl}/k^*_{DB,el} = 0.05$, the force at the target displacement is $F^*_{DB,dTarget} = F^*_{DB,y} + k^*_{DB,pl}\,(d^*_{target} - d^*_{DB,y}) = 196.3$ kN, and the effective stiffness of the equivalent SDOF of the dissipative brace is thus $k^*_{DB,eff} = F^*_{DB,dTarget}/d^*_{target} = 2.3$ kN/mm. Figure 5 (right) reports the idealized force-displacement curves of the SDOF representative of

the frame and of the dissipative braces. Once the hysteretic damping and effective stiffness of the two subsystems are determined, the iterative procedure from step 4) to step 8) is applied until convergence is fulfilled. The final values of hysteretic damping for the two subsystems are $\xi^*_{F,hyst}$ = 17.6% (large Takeda hysteretic model) and $\xi^*_{DB,hyst}$ = 8.8 (ring-spring hysteretic model), and that of the combined system is $\xi^*_{F+DB,hyst}$ = 11.1%. Adding the equivalent viscous damping of the frame $\xi^*_{F,el}$ = 5%, the total damping is $\xi^*_{F+DB,eq}$ = 16.1%. The performance point in the ADRS, considering the elastic spectrum in Figure 3, is $S^*_{d,F+DB}(T^*_{F+DB,eff}, \xi^*_{F+DB,eq})$ = 86.1 mm, which is close enough to the assumed target displacement (the actual roof displacement would be 111 mm rather than 120 mm). The dampers are then distributed along the height according to the proportional criteria proposed by Di Cesare et al. [27].

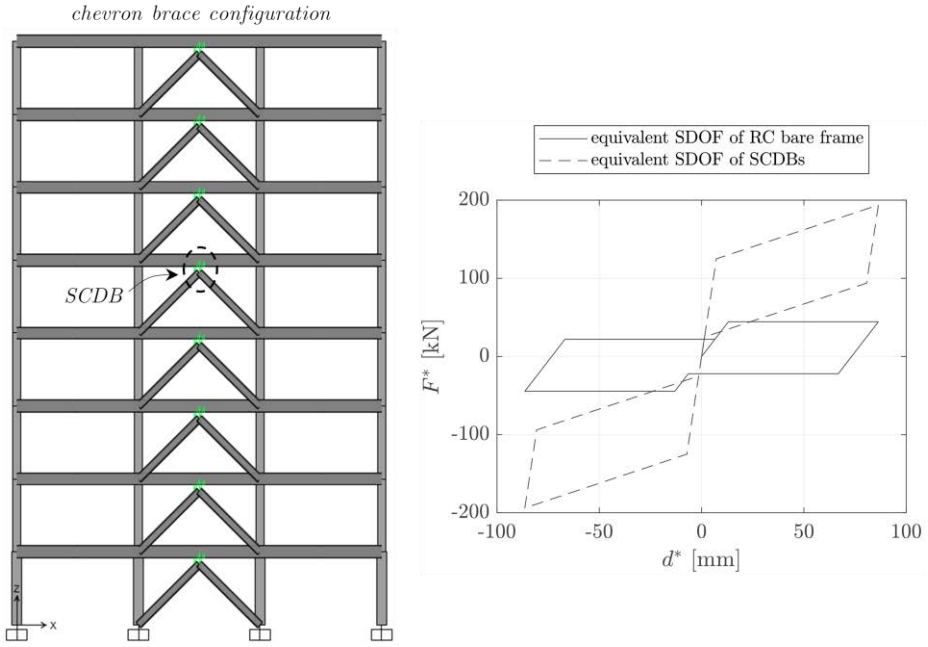

Figure 5: Finite element model of RC frame equipped with SCDBs (left) and force-displacement curves of the equivalent SDOF systems from the design procedure (right)

The SCDBs are modeled through nonlinear link elements available in SAP2000 [30] having a Friction Spring Damper property [30]. The parameters of the link elements introduced in the finite element model reflect the desired hysteretic characteristics of the dissipative braces obtained from the design procedure. Since the target displacement d_{target} = 120 mm assumed in the design procedure is larger than the original deformation capacity of the bare frame $d_{F,u}$ = 37.5 mm, the actual compatibility of such assumed target displacement has been preliminarily verified through a pushover analysis on the RC frame equipped with the designed SCDBs. It can be observed from Figure 6 that the RC frame with SCDBs exhibits a much larger deformation capacity than the bare frame, and also larger than the assumed target displacement. Therefore, it is concluded that the assumed d_{target} is compatible with the deformation capacity of the retrofitted frame. By looking at the plastic hinge status, it is also worth noting that the introduction of the SCDBs has led to a significant modification of the failure mode of the frame, from an undesired soft-storey mechanism (Figure 4) to a more ductile global collapse mechanism in which the lateral deformation resembles the typical first (triangular) modal shape. This is reasonably due to the inherent hardening behavior of the SCDBs (see again Figure 5 right) that efficiently mitigate the displacement demand concentrated in a particular storey level. Indeed, when a particular storey (e.g., the third storey level as shown in Figure 4)

tends to have a larger deformation than the other storeys, the SCDB of this level react with a higher force as the inter-storey displacement increases, thus effectively preventing the occurrence of undesired damage localization and soft-storey mechanisms.

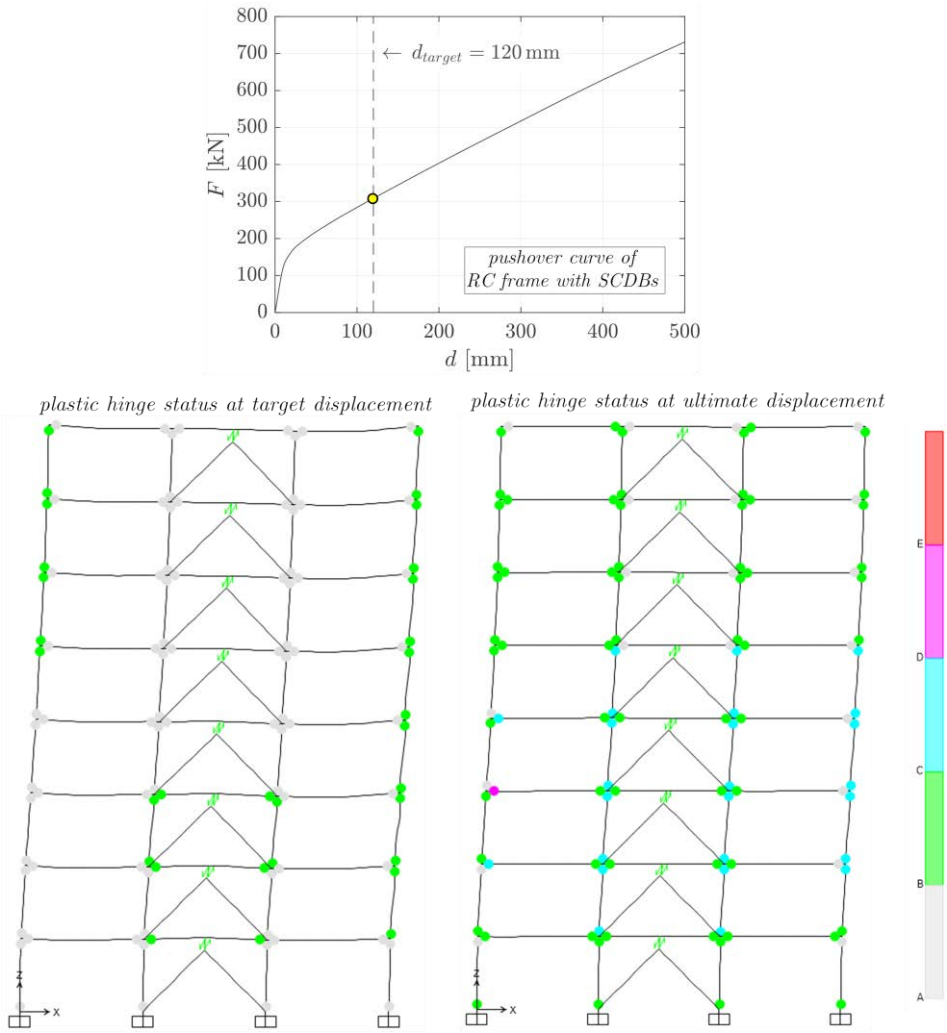

Figure 6: Pushover analysis of RC frame with SCDBs: capacity curve (top) and collapse mechanism (bottom)

A similar linear displacement-based procedure [8] with d_{target} = 120 mm has been applied to design the EPDBs considering the same elastic response spectrum; these braces are implemented in the finite model through the built-in Multi-Linear Plastic property in the nonlinear link elements in SAP2000 [30].

Then, the NLTHAs are performed under the seven selected accelerograms, and the analysis is continued for an extra time of duration 30.0 s (compared to the actual duration of the ground motion record) in order to capture the free vibration response of the RC frame and to investigate the residual displacement d_r at the end of the seismic event. A Newmark constant average acceleration scheme has been adopted for the time integration, and Rayleigh damping scheme is adopted to provide the RC frame with an inherent 5% equivalent viscous damping. The relevant results from NLTHAs are summarized in Table 1 for the seven records as well as the average values of maximum displacement d_{max} and residual displacement d_r. It can be observed that the two classes of dissipative braces, designed for the same target displacement, accomplish a comparable (almost identical) maximum displacement approximately equal to 80 mm. However, a markedly different behavior is observed in terms of recentering capability

of the two classes of dissipative braces: indeed, while the EPDBs exhibit an average residual displacement of almost 20 mm, i.e., approximately one quarter of the maximum displacement, the SCDBs show an excellent recentering capability and negligible values of d_r.

Table 1: Results from NLTHAs on RC frame equipped with EPDBs and SCDBs

	Max displacement d_{max} [mm]		Residual displacement d_r [mm]	
record	*EPDBs*	*SCDBs*	*EPDBs*	*SCDBs*
1	81.9	76.9	9.2	0.6
2	67.0	68.2	3.6	0.0
3	70.4	81.1	13.9	0.1
4	158.7	154.4	96.8	0.3
5	52.0	58.1	2.8	0.1
6	58.6	64.8	1.8	0.0
7	59.2	49.2	1.3	0.1
AVG	78.3	79.0	18.5	0.2

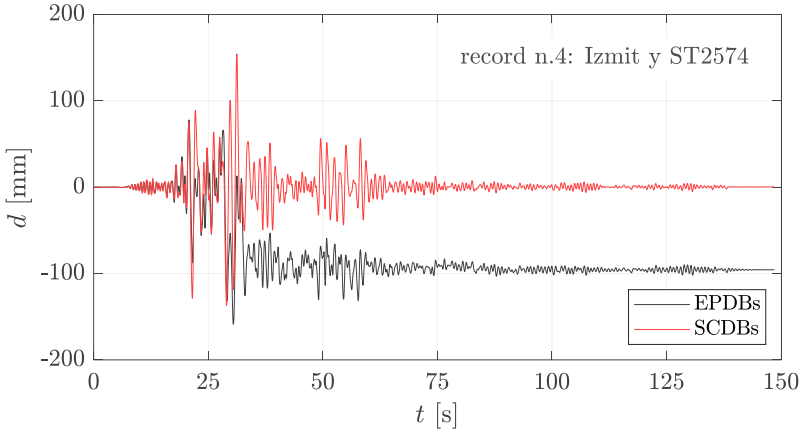

Figure 7: Time-history of the roof displacement response of the RC frame equipped with EPDBs and SCDBs

This result is schematically illustrated for the record n. 4 in Figure 7, where it is clearly noted that, after attaining a comparable peak value (occurring at around t = 30 s), the roof displacement response of the two RC frames considerably deviate with respect to one another. In particular, the RC frame equipped with EPDBs accumulates a permanent displacement of around 100 mm and oscillates around this value, whereas the RC frame equipped with SCDBs is perfectly recentered at the end of the seismic event. This is the main advantage of SCBSs over the EPDBs, especially for repeated seismic events (foreshock, main shock, and aftershock sequences).

From another perspective, one can compare the deformed shape of the RC frame equipped with EPDBs (Figure 8) and with SCDBs (Figure 9) at the time instant corresponding to d_{max} and at the end of the seismic event for the record n. 4 previously commented. Damage concentration in the first two storey levels and a resulting soft-storey mechanism is noted in the RC frame with EPDBs. This large lateral deformation is not recovered anymore and create a permanent shift of the upper six storeys compared to the first two storey levels up to the end of the seismic event. On the contrary, the deformed shape of the RC building with SCDBs at the time instant corresponding to d_{max} resembles a desired triangular profile (first modal shape), with almost uniform distribution of inter-storey drifts at all levels, which is due to the beneficial hardening contribution of the self-centering dampers mentioned above when com-

menting Figure 6. At the end of the seismic event, the RC frame exhibits a perfect recentering behavior and zero residual displacement. Although the peculiar behavior shown for record n. 4 is an extreme case among the seven records here considered (cf. again the results listed in Table 1), it gives a clear idea of the different seismic performance between the EPDBs and the SCDBs when implemented in RC frames like the one considered in this study.

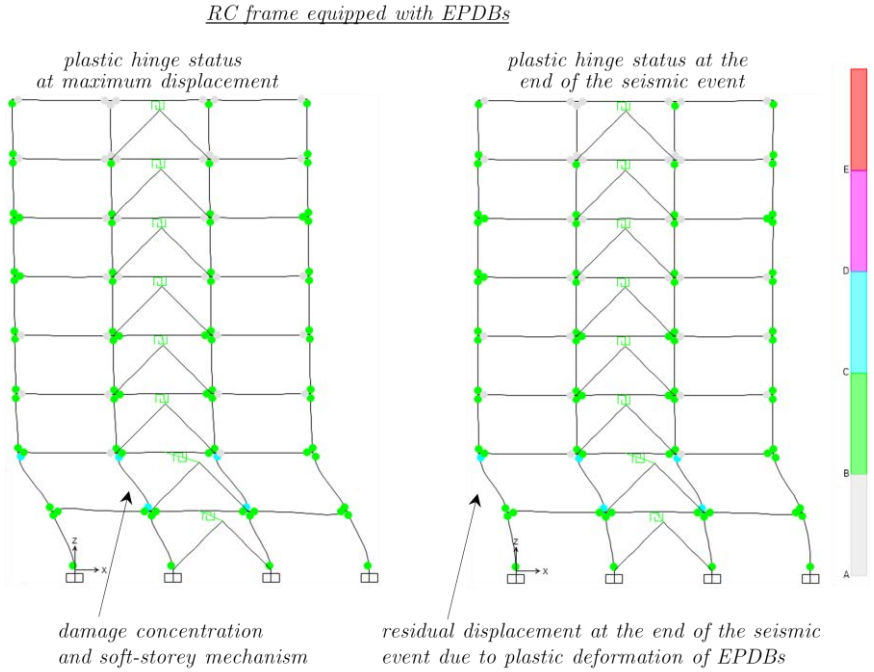

Figure 8: Deformed shape at d_{max} and d_r for RC frame equipped with EPDBs

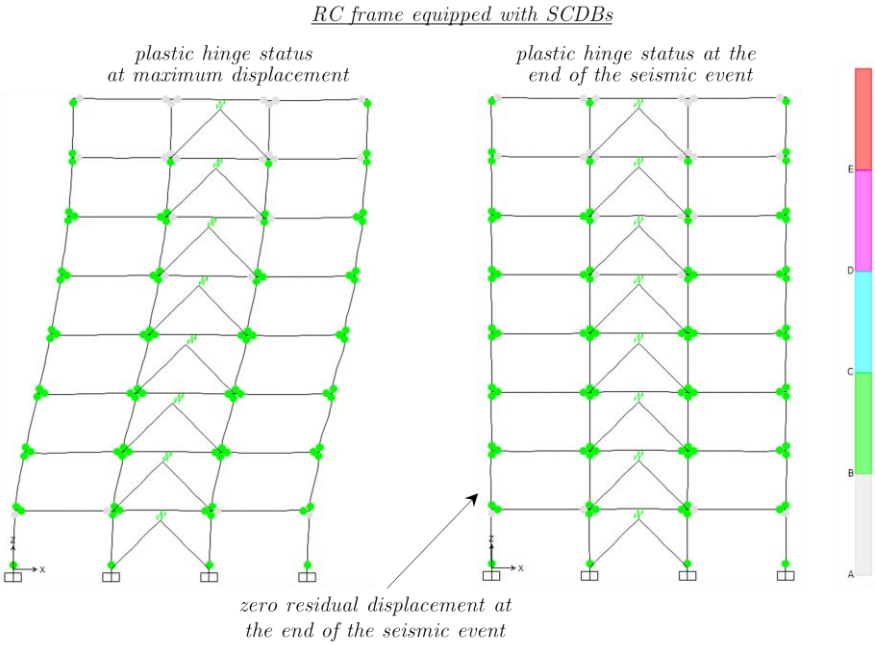

Figure 9: Deformed shape at d_{max} and d_r for RC frame equipped with SCDBs

5 CONCLUSIONS

This contribution has investigated the seismic protection of existing substandard RC frames through SCDBs. A linear displacement-based design procedure for SCDBs implemented in RC framed structures has been illustrated. The procedure addresses two performance requirements, namely the control of the roof displacement that should match a target, predefined value (selected in relationship to the importance of the structure and its intended use), and the good recentering behavior of the structure, quantified via the maximum residual displacement among the ones observed at each storey level after the seismic event.

An RC building representative of the Italian building stock of the 1970s and conceived to resist gravity loads only according to the 1972 Italian codes has been assumed as case study to evaluate the seismic performance of SCDBs, designed according to the above-mentioned procedure. The seismic performance of the RC frame equipped with SCDBs has been numerically evaluated through NLTHAs on a planar model of the RC building under seven natural spectrum-compatible ground motions, and compared to the seismic response of the same frame equipped with EPDBs designed considering the same target displacement for consistency reasons. It has been found that the two classes of dissipative braces accomplish a comparable (almost identical) maximum displacement, in accordance with the design hypothesis. However, a markedly different behavior has been observed in terms of recentering capability of the two classes of dissipative braces: indeed, while the EPDBs exhibit an average residual displacement equal to around one quarter of the maximum average roof displacement, the SCDBs show an excellent recentering capability and zero residual displacement. Moreover, for some of the considered ground motions, damage concentration in the first two storey levels and a resulting soft-storey mechanism has been noted in the RC frame with EPDBs, whereas the deformed shape of the RC frame equipped with SCDBs resembles a desired triangular profile (first modal shape), with almost uniform distribution of inter-storey drifts at all levels.

It is reasonably expected that near-fault records with pulse characteristics and forward-directivity effects might amplify the tendency of exhibiting an asymmetric displacement response, thus producing more marked differences in terms of recentering behavior. A more systematic analysis including both far-field and near-fault records with different seismological characteristics to draw more general conclusions on the seismic performance of the two analyzed dissipative braces certainly deserves further investigation, and is left for future work.

REFERENCES

[1] Italian Ministry of Infrastructures and Transportations (2018) NTC2018. Aggiornamento delle «Norme tecniche per le costruzioni». Decreto 17 Gennaio 2018, Supplemento ordinario alla Gazzetta ufficiale n. 42, 20 February 2018 (In Italian).

[2] European Committee for Standardization. Eurocode 8: design of structures for earthquake resistance—part 1: general rules, seismic actions and rules for buildings. EN 1998-1:2004+A1: 2013. Brussels, Belgium; 2004.

[3] De Domenico, D., Urso, S., Borsellino, C., Spinella, N., & Recupero, A. (2020). Bond behavior and ultimate capacity of notched concrete beams with externally-bonded FRP and PBO-FRCM systems under different environmental conditions. *Construction and Building Materials*, *265*, 121208.

[4] Faleschini, F., Zanini, M. A., Hofer, L., Toska, K., De Domenico, D., & Pellegrino, C. (2020). Confinement of reinforced concrete columns with glass fiber reinforced cementitious matrix jackets. *Engineering Structures*, *218*, 110847.

[5] De Domenico, D., Ricciardi, G., & Takewaki, I. (2019). Design strategies of viscous dampers for seismic protection of building structures: a review. *Soil dynamics and earthquake engineering*, *118*, 144-165.

[6] Idels, O., & Lavan, O. (2021). Optimization-based seismic design of steel moment-resisting frames with nonlinear viscous dampers. *Structural Control and Health Monitoring*, *28*(1), e2655.

[7] De Domenico, D., & Hajirasouliha, I. (2021). Multi-level performance-based design optimisation of steel frames with nonlinear viscous dampers. *Bulletin of Earthquake Engineering*, *19*(12), 5015-5049.

[8] Gandelli, E., De Domenico, D., & Quaglini, V. (2021). Cyclic engagement of hysteretic steel dampers in braced buildings: a parametric investigation. *Bulletin of Earthquake Engineering*, *19*, 5219-5251.

[9] Bruschi, E., Quaglini, V., & Zoccolini, L. (2023). Seismic Upgrade of Steel Frame Buildings by Using Damped Braces. *Applied Sciences*, *13*(4), 2063.

[10] Song, G., Ma, N., & Li, H. N. (2006). Applications of shape memory alloys in civil structures. *Engineering structures*, *28*(9), 1266-1274.

[11] De Domenico, D., Gandelli, E., & Quaglini, V. (2020). Adaptive isolation system combining low-friction sliding pendulum bearings and SMA-based gap dampers. *Engineering Structures*, *212*, 110536.

[12] De Domenico, D., & Gandelli, E. (2021). Advanced modeling of SMA flag-shaped hysteresis for nonlinear time-history analysis in SAP2000. *Journal of Structural Engineering*, *147*(11), 06021004.

[13] Jauhari, M. F., Fardheny, A. F., & Prasetia, D. E. I. (2020). Nonlinear time history analysis of anti seismic device on highway bridges. *Int. J. Adv. Sci. Res. Eng*, *6*(6), 33-39.

[14] Bagheri, H., Hashemi, A., Yousef-Beik, S. M. M., Zarnani, P., & Quenneville, P. (2020). New self-centering tension-only brace using resilient slip-friction joint: Experimental tests and numerical analysis. *Journal of Structural Engineering*, *146*(10), 04020219.

[15] Hashemi, A., Zarnani, P., Masoudnia, R., & Quenneville, P. (2018). Experimental testing of rocking cross-laminated timber walls with resilient slip friction joints. *Journal of Structural Engineering*, *144*(1), 04017180.

[16] Darani, F. M., Zarnani, P., Veismoradi, S., Yousef-beik, S. M. M., Hashemi, A., & Quenneville, P. (2021). Resilient slip friction joint performance: Component analysis, spring model and anti-locking mechanism. *Structures*, 33, 3897-3911.

[17] Hashemi, A., Zarnani, P., Masoudnia, R., & Quenneville, P. (2017). Seismic resistant rocking coupled walls with innovative Resilient Slip Friction (RSF) joints. *Journal of Constructional Steel Research*, *129*, 215-226.

[18] Priestly, M. J. N., Calvi, G. M., & Kowalsky, M. J. (2007). Displacement-based seismic design of structures. *Displacement-Based Seismic Design of Structures, IUSS PRESS, Pavia, Italy*.

[19] Masi, A., & Vona, M. (2012). Vulnerability assessment of gravity-load designed RC buildings: Evaluation of seismic capacity through non-linear dynamic analyses. *Engineering Structures*, *45*, 257-269.

[20] Masi, A. (2003). Seismic vulnerability assessment of gravity load designed R/C frames. *Bulletin of Earthquake Engineering*, *1*, 371-395.

[21] Magenes, G., & Pampanin, S. (2004). Seismic Response of Gravity-Load Design Frame with Masonry Infills. *13th World Conf. Earthq. Eng.,* Vancouver, Canada.

[22] Calvi, G., & Pampanin, G. (2002). Experimental test on a three storey RC frame designed for gravity only, *12th European Conf. Earthq. Eng.,* London, UK, Paper 727.

[23] De Domenico, D., Messina, D., & Recupero, A. (2023). Seismic vulnerability assessment of reinforced concrete bridge piers with corroded bars. *Structural Concrete*, doi: https://doi.org/10.1002/suco.202200378.

[24] P. Zarnani, P. Quenneville, "A Resilient Slip Friction Joint," Patent no. WO2016185432A1, 2016.

[25] Dowell, O. K., Seible, F., & Wilson, E. L. (1998). Pivot hysteresis model for reinforced concrete members. *ACI structural journal*, *95*, 607-617.

[26] Dwairi, H. M., Kowalsky, M. J., & Nau, J. M. (2007). Equivalent damping in support of direct displacement-based design. *Journal of Earthquake Engineering*, *11*(4), 512-530.

[27] Di Cesare, A., Ponzo, F. C., & Nigro, D. (2014). Assessment of the performance of hysteretic energy dissipation bracing systems. *Bulletin of earthquake engineering*, *12*, 2777-2796.

[28] Ministerial Decree 30/5/1972 Design code of reinforced concrete, prestressed concrete and steel structures; 1972 [in Italian].

[29] Iervolino, I., Galasso, C., & Cosenza, E. (2010). REXEL: computer aided record selection for code-based seismic structural analysis. *Bulletin of Earthquake Engineering*, *8*, 339-362.

[30] CSi (2017). Analysis reference manual for SAP2000. SAP2000 version 21, Integrated solution for structural analysis and design. Computers and Structures, Inc., Berkeley, California, USA.

[31] ASCE/SEI Standard 41–17. Seismic evaluation and retrofit of existing buildings. American Society of Civil Engineers, Reston, Virginia, USA; 2017.

[32] Sharma, A., Eligehausen, R., & Reddy, G. R. (2013). Pivot Hysteresis Model Parameters for Reinforced Concrete Columns, Joints, and Structures. *ACI structural journal*, *110*(2).

[33] SEAOC (1995). "Performance-based seismic engineering." in. Vision 2000 committee. Sacramento, CA: Structural Engineers Association of California.

[34] ASCE (2000). FEMA 356 – prestandard and Commentary for the seismic rehabilitation of buildings. Reston, VA: ASCE-American Society of Civil Engineers.